Advanced characterization of electrowetting retroreflectors

Murali K Kilaru, Jia Yang, and Jason Heikenfeld*

Novel Devices Laboratory, Dept. of Elec. & Comp. Engineering, University of Cincinnati, Cincinnati, Ohio 45220, USA

heikenjc@ucmail.uc.edu

Abstract: Electrowetting retroreflectors use a simple and scalable construction, and incorporate an electrically tunable liquid lenslet. By electrically modulating the lenslet geometry, the reflection is switched between retroreflection and scattering. In this paper, we report new capability and characterization, including higher index liquids and contrast ratio as a function of contact angle (θ_V). The reflected intensity is also spatially profiled and reported as a function of view angle. A high contrast ratio of >16X is demonstrated, and methods for further improving performance are discussed. Because the electrowetting retroreflector platform is broad spectrum (VIS-IR), the electrowetting retroreflector may be useful for a large variety of naked eye applications such as safety markings, road-signage, or friend-foe-identification.

© 2009 Optical Society of America

OCIS codes: (080.0080) Geometric optics; (230.0230) Optical devices; (240.0240) Optics at surfaces; (310.0310) Thin films.

References and links

1. H. D. Eckhardt, "Simple Model of Corner Reflector Phenomena," Appl. Opt. **10**(7), 1559–1566 (1971).
2. J. Llyoyd, "A brief history of retroreflective sign face sheet materials," *http://www.rema.org.uk/pdf/history-retroreflective-materials.pdf*.
3. G. C. Gilbreath, W. S. Rabinovich, T. J. Meehan, M. J. Vilcheck, R. Mahon, R. Burris, M. Ferraro, I. Sokolsky, J. A. Vasquez, C. S. Bovais, K. Cochrell, K. C. Goins, R. Barbehenn, D. S. Katzer, K. Ikossi-Anastasiou, and M. Montes, "Large-aperture multiple quantum well modulating retroreflector for free-space optical data transfer on unmanned aerial vehicles," Opt. Eng. **40**(7), 1348–1356 (2001).
4. S. R. William, P. G. Goetz, R. Mahon, L. Swingen, J. Murphy, M. Ferraro, H. R. Burris, C. I. Moore, M. Suite, G. C. Gilbreath, and S. Binari, "45-Mbit/s cat's-eye modulating retroreflectors," Opt. Engin. J. Soc.Photo-Opt. Instrum. Eng. **46**, 10400 (2007).
5. M. K. Kilaru, B. Cumby, and J. Heikenfeld, "Electrowetting retroreflectors: Scalable and wide-spectrum modulation between corner cube and scattering reflection," Appl. Phys. Lett. **94**(4), 041108 (2009).
6. "Reflexite - reflective products - lighting optics, optical engineers, polymer processing," *http://www.reflexite.com/*.
7. F. Mugele, and J. C. Baret, "Electrowetting: from basics to applications," J. Phys. Condens. Matter **17**(28), R705–R774 (2005).
8. B. Berge, and J. Peseux, "Variable focal lens controlled by an external voltage: An application of electrowetting," Eur. Phys. J. E **3**(2), 159–163 (2000).
9. J. Heikenfeld, N. Smith, M. Dhindsa, K. Zhou, M. Kilaru, L. Hou, J. Zhang, E. Kreit, and B. Raj, "Recent Progress in Arrayed Electrowetting Optics," Opt. Photon. News **20**(1), 20–26 (2009).
10. T. B. Jones, "An electromechanical interpretation of electrowetting," J. Micromech. Microeng.1184 (2005).
11. D. A. Arnold, "Method of calculating retroreflector-Array transfer functions," Smithsonian Astrophysical Observatory special report **382,** 1 (1979).
12. P. G. Goetz, W. S. Rabinovich, R. Mahon, L. Swingen, G. C. Gilbreath, J. L. Murphy, H. R. Burris, and M. F. Stell, "Practical considerations of retroreflector choice in modulating retroreflector systems," 2005 Digest of the LEOS Summer Topical Meetings, 49–50 (2005).
13. V. A. Handerek, and L. C. Laycock, "Feasibility of retroreflective free-space optical communication using retroreflectors with very wide field of view," in M. Ross and A. M. Scott, eds. (SPIE), pp. 1–9 (2004.

#113779 - $15.00 USD Received 6 Jul 2009; revised 9 Sep 2009; accepted 9 Sep 2009; published 16 Sep 2009

(C) 2009 OSA

1. Introduction

Retroreflectors reflect light back in the same direction as the light coming from the illumination source [1]. They have numerous applications such as road signs, safety markers, ranging, and surveying [2]. Over the past decade, switchable retroreflectors [3, 4] have been demonstrated for free-space communications. However, these prior approaches utilize microelectromechanical or multiple-quantum well modulation. As a result, the largest application space for retroreflectors, naked eye use, is not practically accessible. We recently reported in a letter [5] an altogether different switchable retroreflector approach that uses a classical corner-cube geometry microreplicated in a polymer substrate. The polymer substrate is metalized just like a conventional large-area retroreflective sheet or film. After metallization, all that is further required is a simple dielectric coating and self assembly of liquid lenslet in each individual hollow corner-cube. Application of voltage modulates electrowetting, lenslet geometry, and thereby the retroreflected intensity. Therefore, a simple and scalable approach is provided that works equally well across the entire visible spectrum. Presented herein are advanced characterizations and improved materials for electrowetting retroreflectors. Characterizations include contrast ratio as a function of voltage, spatial profiling of the retroreflected intensity, and retroreflected intensity as a function of view angle. A high contrast ratio of >16X is demonstrated, and methods for further improving performance are discussed. This work provides further insight into the performance and behavior of electrowetting retroreflectors for naked eye applications such as safety markings, road-signage, or friend-foe-identification.

2. Classical corner-cube retroreflectors

A corner cube retroreflector has three mutually perpendicular reflector faces at a ~54.7° slope (Fig. 1(b)). Incident light is retroreflected after reflecting off symmetrically equivalent points on the faces of the corner cube such as A, B in Fig. 1(b). The loci of all these points that contribute to retroreflection make up the effective aperture of an individual corner cube retroreflector. It is well-known that the effective aperture is only a fraction of the entire triangular aperture of each corner-cube. These effective apertures are the bright regular hexagons in the photo Fig. 1(a). The dark regions labeled in Fig. 1(a) include: (1) the regions towards the edges where only two face reflections occur (dead area); (2) corners between any two faces (corner); (3) reflection of a corner off an opposing face (corner reflections). These bright/dark regions are characteristic of the corner cube retroreflector. Only light rays

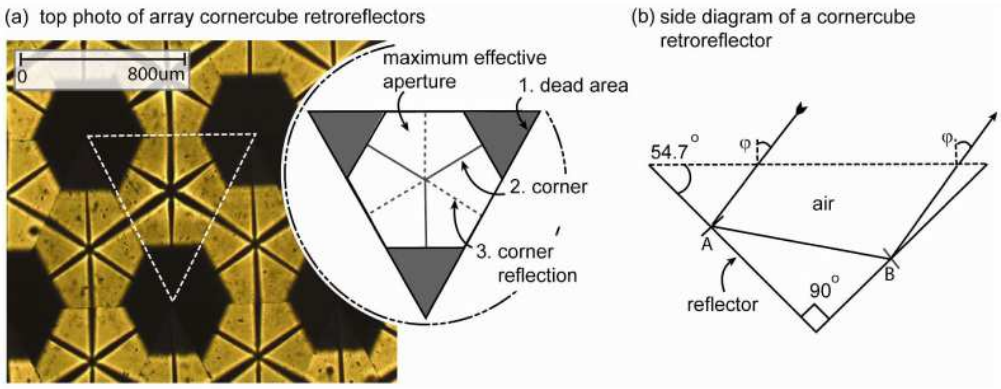


Fig. 1. Hollow corner cube retroreflectors. (a) Photo of arrays of fabricated hollow corner cubes and diagram of the retroreflecting (light) and non-retroreflecting regions (dark). (b) Simple 2D ray trace diagram of a hollow corner cube.

#113779 - $15.00 USD Received 6 Jul 2009; revised 9 Sep 2009; accepted 9 Sep 2009; published 16 Sep 2009
(C) 2009 OSA

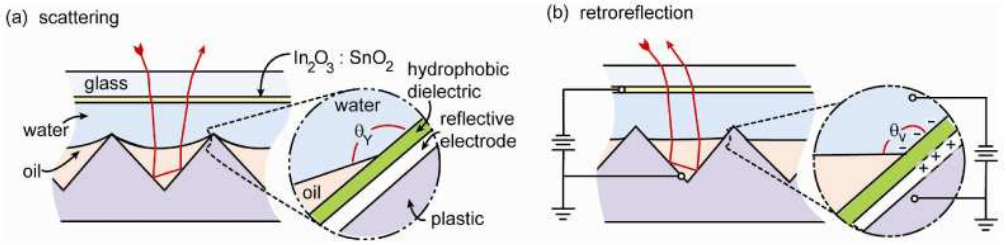


Fig. 2. Side diagram of electrowetting retroreflector modulation. (a) Scattering state (off). (b) Retroreflective state (on).

incident outside these dark areas retroreflect with the same entrance/exit angle (φ, Fig. 1(b)). With high-quality microreplication, only the dark areas at the corner can be minimized, as the dead area at the edges is unavoidable.

3. Electrowetting corner-cube retroreflectors

Electrowetting retroreflectors only require several features beyond a classical corner-cube array. Fabrication is performed as follows with greater detail reported elsewhere [5]. A plastic substrate consisting of ~2500, 800um sized corner cubes are microreplicated using a master from Reflexite Inc [6]. Masters from other companies such as 3M might also be used. These are then conformally coated with a ~300 nm reflective electrode, typically Al, followed by a 5um thick deposition of a Parylene/fluoropolymer hydrophobic dielectric stack (Fig. 2a, inset). These coated hollow corner cubes are then self-assembly dosed with two immiscible liquids, water and oil, with different refractive indices η_w & η_{oil}. In this work we compare two oils of differing refractive index: dodecane (η_{oil}~1.42) and Dow Corning 702 (DC 702) (η_{oil}~1.52), with water being the low index liquid in all experiments (η_w~1.33). The device is sealed with a top-plate and a transparent counter electrode. Surface tension forces cause the liquids to naturally take on a concave lenslet geometry (Fig. 2a). The concavity of the lens is determined by Young's contact angle (θ_Y) for the water on the hydrophobic surface (θ_Y>160°). Typically θ_Y~160°, 140° for water in dodecane and DC 702, respectively. With a co-located illumination source and observation point, the electrowetting retroreflector in this zero-voltage state appears optically scattering.

Electrowetting [7] can be utilized to modulate an optical lens [8], large arrays of devices including display pixels, lens-arrays, prisms [9], and is utilized to create the retroreflective state shown in Fig. 2(b). A voltage is applied between the water and the reflective electrode beneath the hydrophobic dielectric. Charges accumulate at the water-dielectric interface and as a result, the water contact angle (θ_Y) is electromechanically reduced [10] to a new contact angle projection (θ_V). The contact-angle response to voltage is predicted by the so-called electrowetting equation: $cos\theta_V = cos\theta_Y + CV^2/2\gamma$, where C is capacitance per unit area of the hydrophobic dielectric and γ is the interfacial surface tension between the water and the oil. Of particular interest is θ_v equal to or near 125°which creates a flat oil/water mensicus (which is the complement of the side-wall slope ~54.7°). For the flat oil/water meniscus, the lenslet geometry is removed, and the device optically behaves like a classical non-hollow corner cube, except for a minor interference effect that will be discussed in a later section.

4. Characterization of factors affecting contrast ratio

The characterization setup shown in Fig. 3(b) consists of a 632.1nm laser expanded to 0.8 cm^2, incident on the electrowetting retroreflector via a beamsplitter. The retroreflected beam from the electrowetting retroreflector is characterized by a photodetector. The photodetector area and 45 cm distance determines a 0.5° cone that herein is considered to be retroreflected light intensity. The first performance feature to be characterized was contrast ratio vs. contact

#113779 - $15.00 USD Received 6 Jul 2009; revised 9 Sep 2009; accepted 9 Sep 2009; published 16 Sep 2009
(C) 2009 OSA

angle for the cases of dodecane (η_{oil}~1.42) or DC 702 (η_{oi}~1.52) oils. Contrast ratio is the ratio of

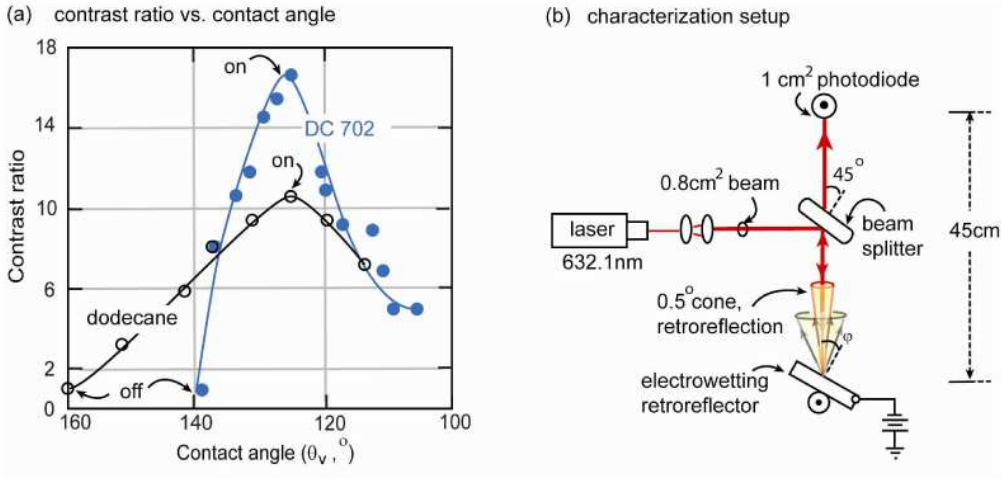


Fig. 3. (a) Plot of contrast ratio vs. θ_V for dodecane and DC 702 oil. (b) Diagram of characterization setup. Percentage error was found to be less than 5%.

retroreflected intensity divided by the scattered intensity at θ_Y. Because light is scattered by a lenslet, the degree of scattering should increase with oil refractive index (η_{oil}) and the deviation of θ_V from 125°. As seen in Fig. 3(a), the retroreflected intensity and contrast ratio increases almost proportionally as θ_V approaches 125°. This trend is common to the devices with both DC 702 and dodecane. However, a sharper transition between scattering and the retroreflected states and a higher contrast ratio (>16), was demonstrated with DC 702. Although DC 702 has a lower θ_Y~140° compared to that of dodecane (θ_Y~160°), it can be interpreted that the higher refractive index of DC 702 has a significant influence.

Further investigation of the dependency of contrast ratio on the contact angle (θ_Y) and oil refractive index(η_{oil}) is explored in the spatial profiling data of Fig. 4. Photos of individual electrowetting corner cubes were obtained using white light illumination through a microscope objective normal to the plane of the substrate. The numerical aperture of the microscope objective is able to capture light reflected within 10° of the surface normal. ImageJ was used to obtain the intensity profile across the surface of an individual electrowetting retroreflector. These photos/intensity profiles illustrate several notable features: (1) expanding dark corner areas in the scattering (off) state; (2) six bright regions near the corner cube center even in the off state; (3) similar shape for the intensity profiles for dodecane and DC 702. All three of these features are worthy of further discussion. First, we turn our attention to the expanding dark corner areas. The dark corner areas are limited by the precision of microreplication and by thin-film coating (i.e. geometrical rounding at the corners). The expanding width of the dark corner in the scattering off state is due to the the curved water/oil interface (lensing). Secondly, we will explain why even in the off state, there are six bright spots near the center of the corner cube. Near the center of the corner cube, and for near normal incidence, the light entrance and exit positions are relatively closely spaced, and therefore light encounters an oil/water meniscus of similar geometry. This undesirable feature of an electrowetting retroreflector fundamentally limits the darkness of the off state. It may be possible to remove this always-retroreflecting area during microreplication. However, doing so will also reduce the maximum retroreflected intensity in the on state of operation. Thirdly, we will address the similarity between the intensity profiles of dodecane vs. DC 702. As shown in Fig. 3(a) the contrast ratio (on/off intensity) for DC 702 is substantially greater than for dodecane. However, one should not expect to see this in the data for Fig. 4, because

#113779 - $15.00 USD Received 6 Jul 2009; revised 9 Sep 2009; accepted 9 Sep 2009; published 16 Sep 2009
(C) 2009 OSA

the collection angle of the microscope objective is 10°, much largerthan the 0.5° used to measure contrast ratio in Fig. 3.

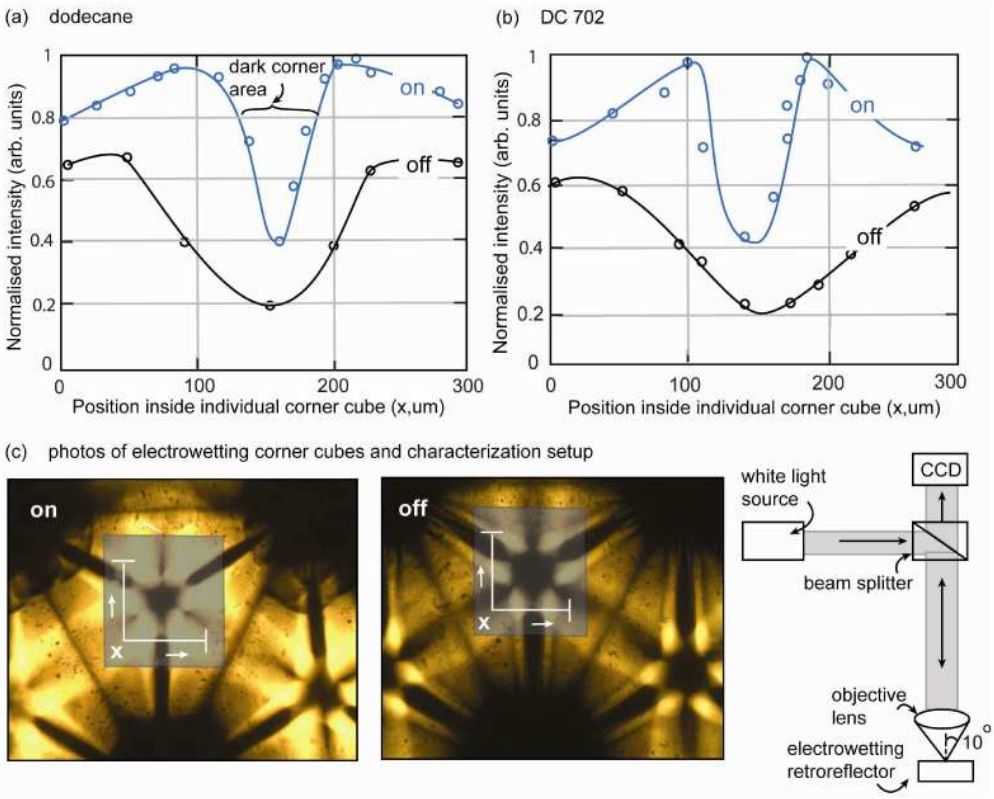


Fig. 4. On and off intensity plots of electrowetting corner cube for (a) dodecane oil and (b) DC 702 oil. Photos of the device in the on and off states, along with the characterization setup, is shown in (c). Percentage error was found to be less than 5%.

5. Characterization of viewing angle

Viewing angle is the maximum incidence angle($\varphi_{1/2}$) about the normal to the retroreflector plane over which the retroreflected light is half the maximum possible retroreflected intensity ($\varphi_{1/2}$). The retroreflected intensity of a hollow corner cube retroreflector decreases as the incidence angle increases. To visualize this effect, shown in Fig. 5 are photos of the arrays of hollow corner cubes that are taken through a microscope objective at various external incident angles (φ_{ext}=0°, 15°, 30°). The bright regular hexagons shown in Fig. 5(a) present the largest possible effective aperture for retroreflection at normal incidence (φ_{ext}=0°) and correspondingly provide the highest retroreflected intensity I(0°)[11]. Theoretically, the retroreflected intensity decreases to half the maximum at $\varphi_{1/2}$~ ±10° for a hollow corner cube retroreflector [12]. The decrease in intensity with increasing incidence angle is predicted by Eq. (1) [13].

$$\frac{I(\varphi_{ext})}{I(0^0)} = \left(1-\sqrt{2}\tan(\varphi_{int})\right)^2\left[1-\frac{\sqrt{2}}{3}\tan(\varphi_{int})\right]^2\cos^2(\varphi_{ext}) \qquad (1)$$

Where, $\varphi_{int}=\sin^{-1}[\sin(\varphi_{ext})/\eta_{oil}]$; Filling the hollow corner cubes with refractive media (η_{oil}>~1.4), results in increasing the viewing angle ($\varphi_{1/2}$) to >15°. This is because the external incidence angle (φ_{ext}) is reduced internally ($\varphi_{int} < \varphi_{ext}$) via refraction [1, 12].

#113779 - $15.00 USD Received 6 Jul 2009; revised 9 Sep 2009; accepted 9 Sep 2009; published 16 Sep 2009
(C) 2009 OSA

To validate the increase of viewing angle by incorporation of high index oils, electrowettingretroreflectors were characterized for retroreflected intensity vs. incidence angle (φ_{ext}) in theretroreflecting state (θ_V~125°) using the setup previously shown in Fig. 3b. Three differentelectrowetting retroreflector devices were characterized: (a) η_{oil}~1 (hollow corner cube, air);

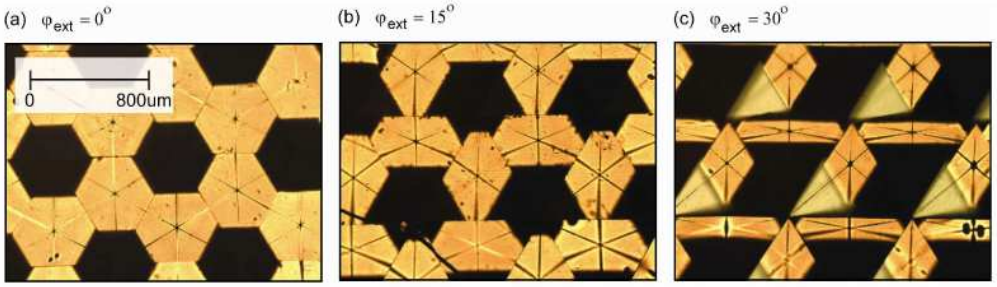


Fig. 5. Photos of arrays of hollow corner cube retroreflectors showing the decrease of the effective aperture with increase in incidence angle. (a) φ_{ext}=0°. (b) φ_{ext}=15°. (c) φ_{ext}=30°.

(b) η_{oil} ~1.42 (dodecane); (c) η_{oil} ~1.52 (DC 702). The blue line in Fig. 6 represents the trend line for experimental data against the expected behavior from Eq. (1) represented by the black line. As shown in Fig. 6, increased viewing angle ($\varphi_{1/2}$) was obtained for devices containing the higher index oils. This effect was expected. However, also visible in Fig. 6 is a single peak in intensity at small incidence angle, not the expected peak at zero incidence angle. This is speculated to be a result of interference arising from electrowetting hydrophobic dielectric stack (Fig. 2). It is clearly not due to the liquids or the top sealing plate, because even the device which has no liquids (Fig. 6(a)) shows this peak. In thin film interference, the intensity of the refracted/reflected light depends on angle of incidence. For the device (a) the maximum intensity is observed at ~5° (Fig. 6), which translates to incidence angle on the thin film coating of ~49.75° (54.75° -φ_{ext}). Now, as the refractive index of the filling medium of the corner cube is increased to η_{oil}~1.42, 1.52, the external incidence angle φ_{ext} is reduced to φ_{int}. This should therefore, shift the interference peak to larger angles (theoretical φ_{ext} ~ 7° for η_{oil}=1.42, ~8° for η_{oil}=1.52), which are close to experimentally observed values from Fig. 6 (φ_{ext} ~9° for η_{oil}=1.42, ~10° for η_{oil}=1.52). Lastly, we should note that the high contrast ratios observed (~10 and ~16 for dodecane, DC 702 respectively) were for normal light incidence. Therefore a slightly higher (~10-20%) contrast ratio is expected to be achieved at the peak angles shown in Fig. 6.

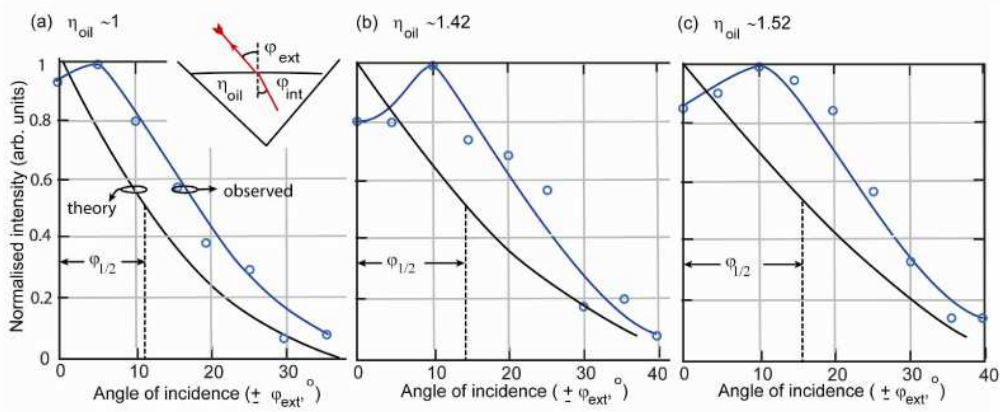


Fig. 6. Field of view. (a) Air η_{oil}~1. (b) Dodecane η_{oil}~1.42. (c) DC 702 η_{oil}~1.52. Percentage error was found to be less than 5%.

#113779 - $15.00 USD Received 6 Jul 2009; revised 9 Sep 2009; accepted 9 Sep 2009; published 16 Sep 2009
(C) 2009 OSA

Acknowledgements

The authors acknowledge partial financial support for this work including Army CERDEC (S. Haught), Air Force Research Labs (R. Naik), AFOSR Young Investigator Award #06NE223 (K. Reinhardt), and an NSF CAREER Award #0640964 (EPDT).

#113779 - $15.00 USD Received 6 Jul 2009; revised 9 Sep 2009; accepted 9 Sep 2009; published 16 Sep 2009
(C) 2009 OSA